Received: 18 November 2022 | Accepted: 22 December 2022

DOI: 10.1111/1759-7714.14791

ORIGINAL ARTICLE

WILEY

MiR-138-5p suppresses the progression of lung cancer by targeting SNIP1

Jiaen Wu[1,2] | Xuejia Han[1,2] | Xiancong Yang[1] | Youjie Li[1] | Yan Liang[1] | Guangbin Sun[1] | Ranran Wang[1] | Pingyu Wang[1] | Shuyang Xie[1] | Jiankai Feng[2] | Hongfang Sun[1]

[1]Department of Biochemistry and Molecular Biology, Binzhou Medical University, Yantai, China

[2]Department of Laboratory Medicine, Yantai Affiliated Hospital of Binzhou Medical University, Yantai, China

Correspondence
Hongfang Sun and Shuyang Xie, Department of Biochemistry and Molecular Biology, Binzhou Medical University, Yantai, Shandong, 264003, China.
Email: sunhongfang924@163.com and shuyangxie@aliyun.com

Jiankai Feng, Department of Laboratory Medicine, Yantai Affiliated Hospital of Binzhou Medical University, Yantai, Shandong, 264100, China.
Email: 15154502685@163.com

Funding information
National Natural Science Foundation of China, Grant/Award Number: 82002604

Abstract

Background: MicroRNAs (miRNAs) play crucial roles in the development of various cancers. Here, we aimed to evaluate the roles of miR-138-5p in lung cancer progression and the value of miR-138-5p in lung cancer diagnosis.

Methods: Quantitative real-time PCR was performed to examine the expressions of miR-138-5p and smad nuclear interacting protein 1 (SNIP1) mRNA. The diagnostic value of miR-138-5p was analyzed using receiver operating characteristic (ROC) curve analysis, sensitivity, and specificity. We explored the effect of miR-138-5p on cell proliferation and metastasis by CCK-8, colony formation, wound healing and transwell assays. Western blot was employed to detect the protein expression of SNIP1 and related genes. Lung cancer cell growth was evaluated in vivo using xenograft tumor assay.

Results: MiR-138-5p was decreased in the serum of patients with non-small cell lung cancer (NSCLC) and in NSCLC cells and tissues. The area under the ROC curve of serum miR-138-5p in the diagnosis of NSCLC was 0.922. This finding indicates the high diagnostic efficiency for lung cancer. MiR-138-5p suppressed but its inhibitor promoted cell proliferation and migration compared with control treatment in vitro and in vivo. MiR-138-5p directly binds to the 3′-untranslated region of SNIP1 and negatively regulated the expression of SNIP1, thereby inhibiting the expression of cyclin D1 and c-Myc. Moreover, overexpression of SNIP1 rescues the miR-138-5p-mediated inhibition in NSCLC cells.

Conclusions: The results suggested that miR-138-5p suppressed lung cancer cell proliferation and migration by targeting SNIP1. Serum miR-138-5p is a novel and valuable biomarker for NSCLC diagnosis.

KEYWORDS
biomarker, lung cancer, miR-138-5p, SNIP1, tumor suppressor

INTRODUCTION

Lung cancer is one of the most common malignant tumors that seriously threaten human health. At present, the morbidity of lung cancer is increasing year by year.[1] Non-small cell lung cancer (NSCLC), the most prevalent type of lung cancer, is characterized by insidious onset, chemotherapy resistance, and poor treatment effect.[2] NSCLC mainly includes lung adenocarcinoma (LUAD) and lung squamous cell carcinoma (LUSC). Therefore, further investigation of the molecular mechanism of NSCLC progression is urgently needed for the development of new effective therapeutic

Jiaen Wu and Xuejia Han contributed equally to this work.

strategies and to improve the survival rate of lung cancer patients.

MicroRNAs (miRNAs) are a class of short RNAs consisting of 19–25 nucleotides. MiRNAs can regulate the expression of multiple genes by binding to the 3′-untranslated region (3′-UTR) of target mRNAs.[3] The dysregulation of miRNAs has been demonstrated in human cancers, and is involved in various physiological processes of tumor cells, such as proliferation, differentiation, cell cycle, apoptosis, metabolism, and cell signaling.[4,5] In recent years, several studies indicate that miRNAs can be useful as diagnostic biomarkers for NSCLC.[6,7] Further insight into the role and molecular mechanism of miRNAs for NSCLC may contribute to understanding the development and progression of NSCLC.

The dysregulation of miR-138-5p plays important roles in the carcinogenesis of lung cancer.[8–10] The expression of miR-138-5p in NSCLC tissues was significantly downregulated compared with that in adjacent tissues.[9] Further, serum miRNAs can be employed as biomarkers for the detection of lung cancer.[11–14] The role and mechanism of miR-138-5p in lung cancer tumorigenesis and its diagnostic value as a diagnostic biomarker of lung cancer needed to be further investigated. In this study, we analyzed the expression of miR-138-5p in lung cancer serum samples to determine the diagnostic value of miR-138-5p as a biomarker of lung cancer and identify whether smad nuclear interacting protein 1 (SNIP1) is a direct target of miR-138-5p in the regulation of tumor progression.

METHODS

Patient serum samples

A total of 18 pairs of lung cancer serum samples and matched normal serum samples were collected from the Yantai Affiliated Hospital of Binzhou Medical University (Yantai, China) between November, 2020 and October, 2022. The serum samples were collected according to standard phlebotomy procedures. The samples were centrifuged at 900 *g* for 10 min, transferred into RNase-free centrifuge tubes, and stored at −80°C until analysis.

Cell lines and cell culture

The human normal epithelial lung cell line BEAS-2B and the human lung cancer cell lines A549, NCI-H1975 and PC-9 were purchased from the Shanghai Institute of Cell Biology, China. A549 and H1975 cells were cultured in RPMI 1640 medium (Gibco, Thermo Fisher Scientific) containing 10% fetal bovine serum supplemented with 1% streptomycin and penicillin. BEAS-2B and PC-9 cells were cultured in DMEM medium (Gibco, Thermo Fisher Scientific) supplemented with 10% fetal bovine serum (AusGenex) and penicillin–streptomycin (Gibco, Thermo Fisher Scientific). Cells were cultured at 37°C in a humidified incubator with 5% CO_2.

RNA extraction and RT-qPCR

The microRNA was extracted from 200 µl serum using a serum RNA extraction kit (BioTeke). RNAs were isolated from cell lines by the TRIzol reagent (Invitrogen). RNA was reverse transcribed into first strand cDNA using PrimeScript RT Master Mix (Takara Bio, Inc.). Moreover, qPCR with SYBR Premix Ex Taq II (Thermo Fisher Scientific Inc.) was performed using the following thermocycling conditions: 50°C for 2 min followed by 40 cycles of 95°C for 2 min, 95°C for 15 s, and 60°C for 20 s. GAPDH or 5 S rRNA served as internal controls to normalize the expression levels of mRNAs or miRNAs, respectively. The primer sequences were as follows: SNIP1-forward, 5′-GAAACCGAAGTCCTCAC CAC-3′; SNIP1-reverse, 5′-TTCCTGTTCTGATGGTTCCC-3′; GAPDH-forward, 5′-AATGGACAACTGGTCGTGGAC-3′; GAPDH-reverse, 5′-CCCTCCAGGGGATCTGTTTG-3′; miR-138-5p-forward, 5′-AGTCTGGTGTTGTGA ATCAGGC-3′; miR-138-5p-reverse, 5′-AACATGTACAGTCCATGGATG-3′; 5 S rRNA-forward, 5′-GCCATACCACCCTGAACG-3′; 5 S rRNA-reverse, 5′-AACATGTACAGTCCATGGATG-3′.

Plasmid constructs and cell transfection

Full length human wild-type SNIP1 cDNA was amplified and cloned into pcDNA3.1 (−) plasmid. The primer sequences were as follows: forward, 5′-ATGAAGGCGGT GAAGAGCGAACG-3′ and reverse, 5′-CTAGCTGTCA GACACTTCTTCCT-3′. MiR-138-5p mimic, miR-138-5p inhibitor, and negative control were purchased from Gene Pharma (Shanghai Gene Pharma Co., Ltd.). Cell transfection was performed using the Lipofectamine 2000 transfection reagent (Invitrogen) following the manufacturer's instructions.

Cell proliferation assay

Cell proliferation was measured using a cell counting kit-8 (CCK-8; Dojindo Molecular Technologies, Inc.). Briefly, 1000 cells were plated in each well of a 96-well plate. After 24, 48, and 72 h, 10 µl CCK-8 solution was added into each well and the cells were incubated for 2 h at 37°C. Finally, the absorbance of each well at 450 nm was detected using a microplate reader (Bio-rad laboratories, Inc.).

Colony formation assay

Cell colony formation ability was measured using a colony formation assay. The transfected cells were cultured in the six-well plates for 24 h, and then the cells were counted.

Approximately 1×10^3 cells were inoculated in a 10 cm dish and cultured for 14 days to allow colony formation. Cell colonies were fixed with 4% paraformaldehyde and stained with crystal violet. Finally, the stained colonies were photographed and counted for statistical analysis.

Transwell assay

Transwell migration assay was performed with transwell chambers (Corning). Briefly, 5×10^4 transfected cells were seeded into the upper chamber, and RPMI-1640 medium supplemented with 25% FBS was added to the lower chamber. Following 24 h of incubation, the chamber was fixed with 4% formaldehyde and stained with crystal violet. The number of migratory cells was determined by counting five randomly selected fields under a microscope (Leica DM6000B).

Wound healing assay

Cell migratory capacity was measured using a wound healing assay. The transfected cells were plated into six-well plates and cultured to 100% confluence. A straight linear scratch wound was then created in the cell monolayer using a 200 μl pipette tip, and the cells were washed with phosphate buffered saline (PBS). The cells were subsequently cultured in serum-free medium. The wound healing distance was measured at 0, 24, and 48 h, and the wound areas were photographed using an alive cell workstation (EVOS M7000; Thermo Fisher Scientific). The percentage of the wound closure representing the migration ability of the cells was measured using ImageJ software.

Western blot

Total protein was extracted from transfected cells using RIPA lysis buffer (Beyotime Biotechnology, China) according to the manufacturer's instructions. The cell lysate was then centrifuged at 13500 *g* for 15 min at 4°C. The supernatant was collected and boiled with the SDS loading buffer. The protein samples were separated by SDS-polyacrylamide gel electrophoresis (SDS-PAGE) and transferred to polyvinylidene fluoride (PVDF) membranes (Millipore). The membranes were blocked with 5% nonfat dry milk and incubated with primary antibodies SNIP1 (anti-SNIP1, 1:800, 14950-1-AP, Proteintech), Cyclin D1 (anti-cyclin D1, 1:800, BS1741, Bioworld), Vimentin (anti-vimentin, 1:800, BS1491, Bioworld), E-cadherin (anti-E-cadherin, 1:800, BF0219, Affinity), c-Myc (anti-c-Myc, 1:1000, 10828-1-AP, Proteintech), and GAPDH (anti-GAPDH, 1:800, AP0063, Bioworld), followed by reaction with HRP-conjugated secondary antibodies (1:6000, Proteintech). Finally, the protein bands were visualized using enhanced chemiluminescence (ECL) reagent (Beyotime Biotechnology).

Luciferase assay

The primer sequences for the wild-type SNIP1-3′UTR were as follows: forward, 5′-TAGTAGAGATGGGGTTTCACCATATTGGCC-3′, reverse, 5′-GGATATGACTAGGAAGAGACTCAAGGGGTA-3′. For the luciferase assay, A549 and H1975 cells were transfected with the luciferase vectors and miR-138-5p using lipofectamine 2000 (Invitrogen). After 24 h, the luciferase activity of the transfected cells was measured by chemiluminescence detector (Infinite 200 pro, Tecan, Switzerland), and the results were normalized against the β-galactosidase activity. Three replicate samples were set up for each group, and each experiment was assayed in triplicate.

In vivo tumorigenesis assays

The cancer cell xenograft in null mice was performed as described previously.[15] For this study, 4-6-week-old female BALB/c nude mice were purchased from Hangzhou Ziyuan Experimental Animal Technology Co., Ltd. The mice were procured and the study was conducted according to the guidelines as well as protocol approved by the Animal Experimentation Ethics Committee of Binzhou Medical University, China. 1×10^7 cells were injected subcutaneously into the flank of the nude mice. The mice were checked daily for tumor appearance by palpation. Tumor volumes were measured every 2 days. After 32 days, the mice were sacrificed, and the subcutaneous tumors were removed, weighed, and photographed.

Statistical analysis

All experiments were repeated at least three times. Statistical analyses were performed using GraphPad Prism (version 8.2.1; GraphPad Software, Inc.). Data are presented as means ± SD. Differences between two groups were compared using Student's *t*-test. Differences among multiple groups were calculated using ANOVA. $p < 0.05$ indicated a statistically significant difference. *; **; or *** corresponded to $p < 0.05$; $p < 0.01$; or $p < 0.001$, respectively.

RESULTS

Serum miR-138-5p is a potential diagnostic marker for NSCLC

MiR-138-5p was characterized as a tumor suppressor in bladder cancer,[16,17] colorectal cancer,[18] breast cancer,[19] and hepatocellular carcinoma.[20,21] To determine the diagnostic value of miR-138-5p as a biomarker of lung cancer, we investigated miR-138-5p expression in 18 lung cancer serum samples and matched adjacent normal serum samples through qRT-PCR. The miR-138-5p expression was

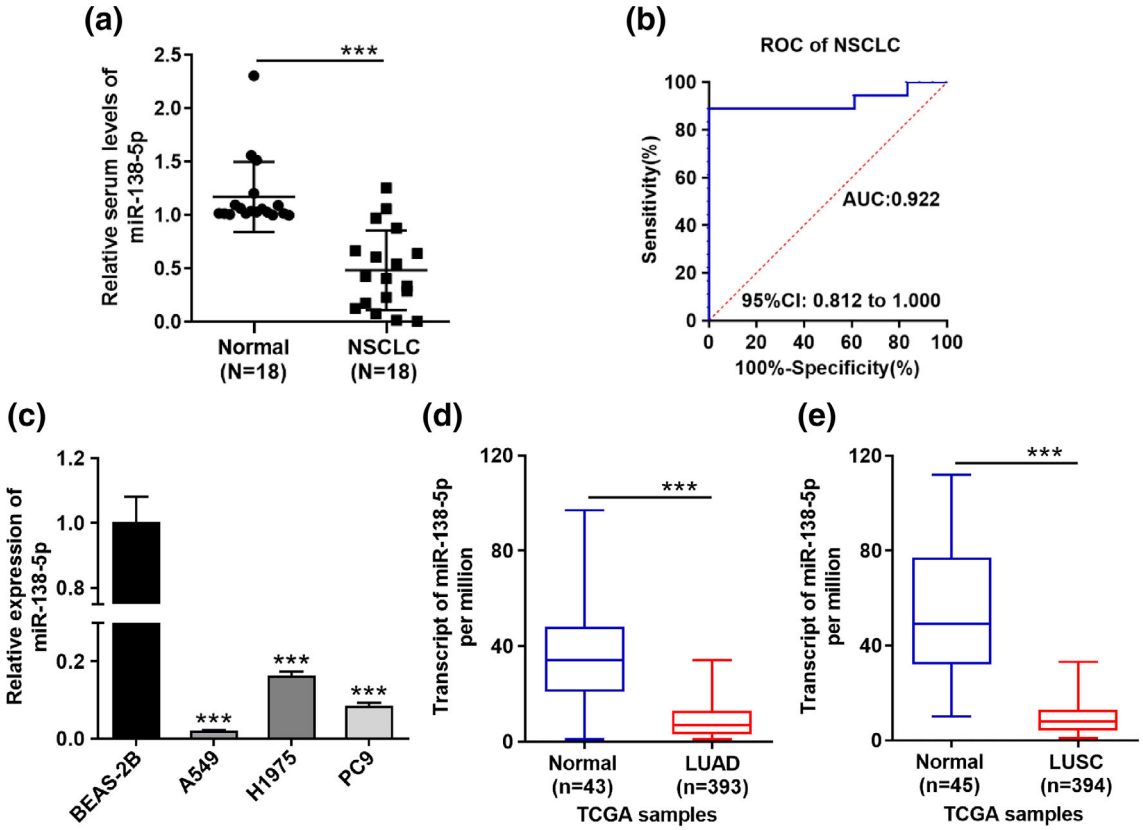

FIGURE 1 MiR-138-5p is downregulated in lung cancer. (a) RT-qPCR was performed to evaluate the expression of miR-138-5p in 18 lung cancer serum samples and matched adjacent normal serum samples. (b) The receiver-operating curve (ROC) curve of serum miR-138-5p was analyzed in non-small cell lung cancer (NSCLC) patients. (c) Relative expression of miR-138-5p in NSCLC cells. (d, e) miR-138-5p levels in lung adenocarcinoma (LUAD, $n = 393$) compared with normal controls ($n = 43$) and in lung squamous cell carcinoma (LUSC, $n = 394$) compared with normal controls ($n = 45$) from the cancer genome atlas (TCGA), respectively. All data are presented as the mean ± SD of three independent experiments (***$p < 0.001$).

significantly reduced in the lung cancer serum samples compared with normal controls ($p < 0.001$) (Figure 1a). Receiver-operating characteristic (ROC) curve analysis to evaluate the diagnostic value of serum miR-138-5p for NSCLC patients revealed a cutoff value of 1.018, with the highest specificity and sensitivity. Thus, serum miR-138-5p levels may be a valuable biomarker for distinguishing lung cancer patients from healthy controls, with an area under the ROC curve (AUC) of 0.922 (95% confidence interval [CI]: 0.812–1.000; Figure 1b).

MiR-138-5p is downregulated in lung cancer cell lines and tissues

Subsequently, we detected the level of miR-138-5p in normal epithelial lung cell lines BEAS-2B, A549, H1975, and PC-9. Lower miR-138-5p expression was noted in NSCLC cell lines compared with BEAS-2B cells (Figure 1c). Data from the cancer genome atlas (TCGA) also indicated that miR-138-5p expression was significantly decreased in lung adenocarcinoma tissues ($n = 393$) compared to the normal controls ($n = 43$, $p < 0.001$) (Figure 1d) and in lung squamous cell carcinoma tissues ($n = 394$) compared to the normal controls ($n = 45$, $p < 0.001$) (Figure 1e). These results indicated that miR-138-5p may suppress the progression of lung cancer.

MiR-138-5p inhibited the growth of lung cancer cells

MiR-138-5p is reported to inhibit tumor progression,[22] but its role in NSCLC remains unclear. To investigate the potential biological function of miR-138-5p in NSCLC, miR-138-5p mimic or miR-138-5p inhibitor was transfected into A549 and H1975 cells. MiR-138-5p expression was upregulated in NSCLC cells transfected with miR-138-5p mimic compared with NC mimic (Figure 2a,b), and miR-138-5p expression was downregulated in NSCLC cells transfected with miR-138-5p inhibitor compared with NC inhibitor (Figure 2a,b).

CCK-8 assay was performed to evaluate the effects of increased miR-138-5p levels on cell viability. MiR-138-5p significantly suppressed the proliferation of NSCLC cells compared to NC mimic (Figure 2c,d). However, miR-138-5p inhibitor treatment promoted A549 and H1975 cell proliferation compared with control treatment (Figure 2e,f). Cell proliferation in miR-138-5p-overexpressing and control

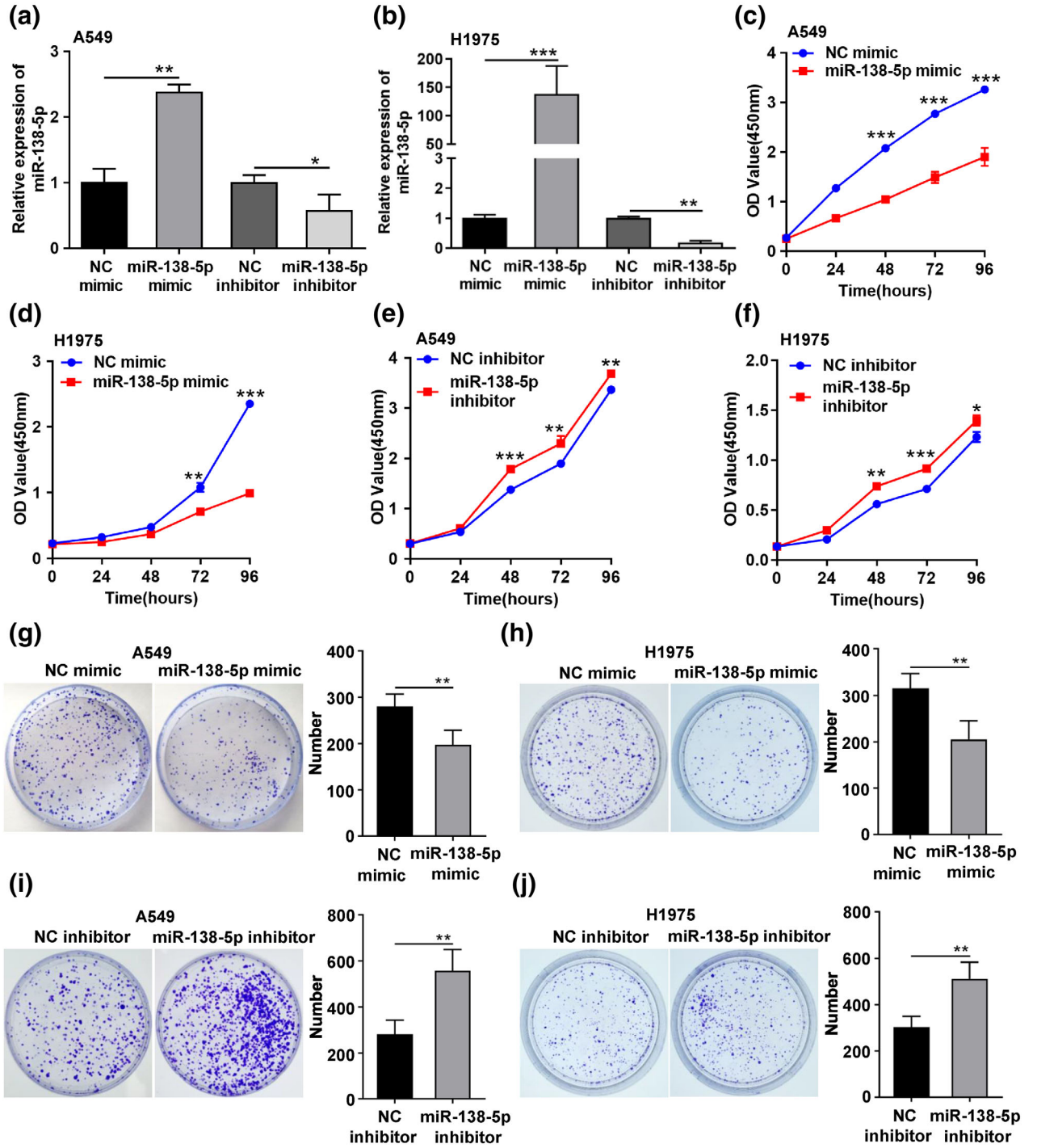

FIGURE 2 MiR-138-5p inhibited the growth of lung cancer cells. (a, b) Relative expression of miR-138-5p in A549 and H1975 cells transfected with NC mimic, miR-138-5p mimic, NC inhibitor or miR-138-5p inhibitor. (c–f) The cell counting kit-8 (CCK-8) viability assay was performed at 24, 36, 48, and 96 h after the A549 and H1975 cells were transfected with miR-138-5p mimic, miR-138-5p inhibitor, or corresponding negative control RNA (NC mimic and NC inhibitor). (g–j) Colony formation of A549 and H1975 cells transfected with NC mimic, miR-138-5p mimic, NC inhibitor or miR-138-5p inhibitor. Left panel: Representative image. Right panel: Quantitative analysis. (c, d, g, h) Overexpression of miR-138-5p suppressed the growth of A549 and H1975 cells. (e, f, i, j) miR-138-5p inhibitor promoted the proliferation of A549 and H1975 cells. All data are presented as the mean ± SD of three independent experiments (*$p < 0.05$; **$p < 0.01$; ***$p < 0.001$).

cells were also determined by colony formation. As shown in Figure 2g,h, miR-138-5p overexpression repressed cell proliferation compared with the control cells. Clone formation assay also confirmed that miR-138-5p inhibitor promoted the proliferation of A549 and H1975 cells compared to NC inhibitor (Figure 2i,j). A series of experiments suggested that miR-138-5p inhibited lung cancer progression.

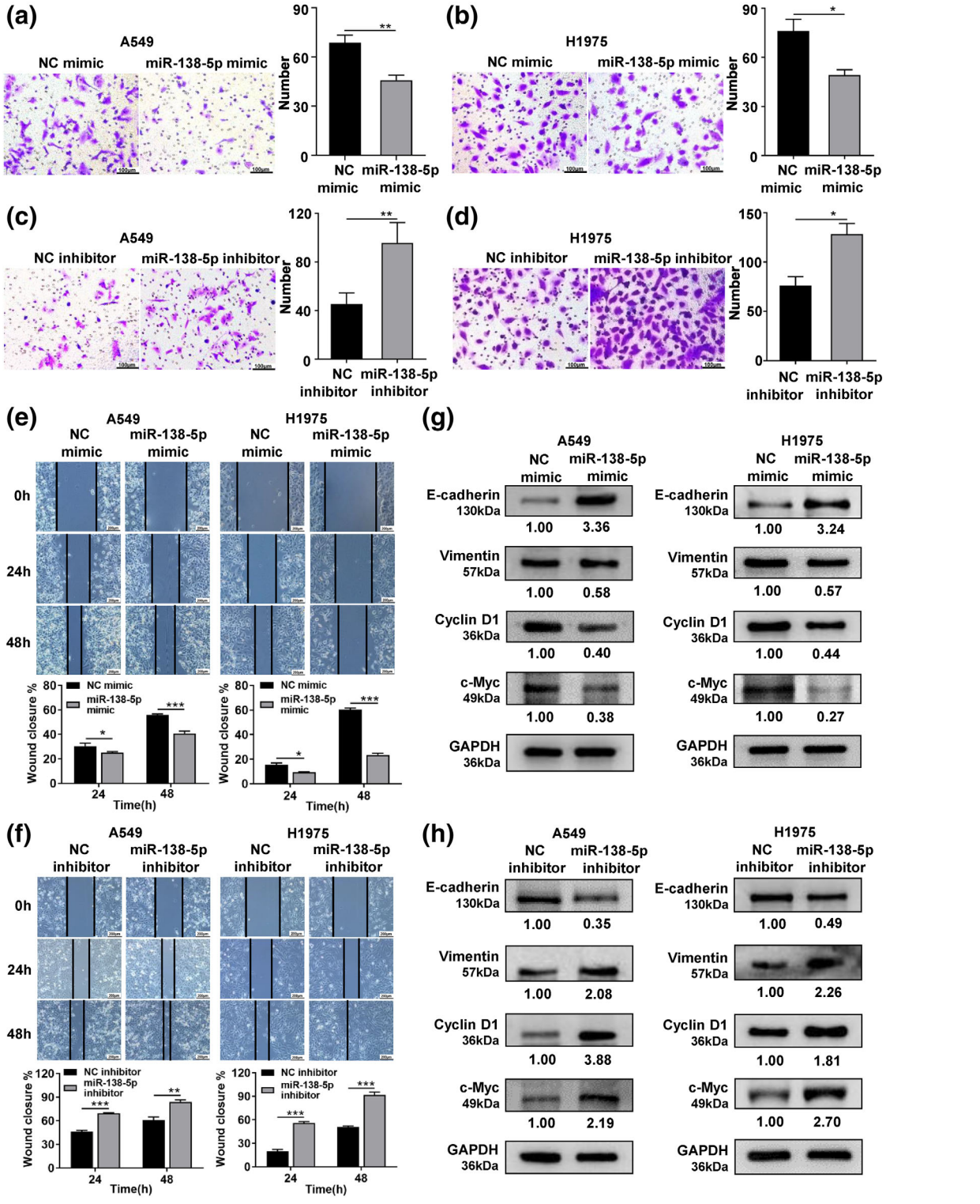

FIGURE 3 MiR-138-5p suppressed the migration of lung cancer cells. (a–d) Transwell analysis of A549 and H1975 cells transfected with miR-138-5p mimic, miR-138-5p inhibitor or corresponding negative control RNA (NC mimic and NC inhibitor). Left panel: Representative image. Right panel: Quantitative analysis. All data are presented as the mean ± SD of three independent experiments (*$p < 0.05$; **$p < 0.01$). (e, f) Wound healing assay of A549 and H1975 cells treated with equal amounts of miR-138-5p mimic, miR-138-5p inhibitor or corresponding negative control RNA (NC mimic and NC inhibitor). Top panel: Representative image. Bottom panel: Quantitative analysis of wound closure. All data are presented as the mean ± SD of three independent experiments (*$p < 0.05$; **$p < 0.01$; ***$p < 0.001$). (a, b, e) Overexpression of miR-138-5p suppressed the migration of A549 and H1975 cells. (c, d, f) MiR-138-5p inhibitor promoted the migration of A549 and H1975 cells. (g, h) Expression levels of E-cadherin, vimentin, cyclin D1, c-Myc, and GAPDH in A549 and H1975 cells transfected with NC mimic, miR-138-5p mimic, NC inhibitor or miR-138-5p inhibitor.

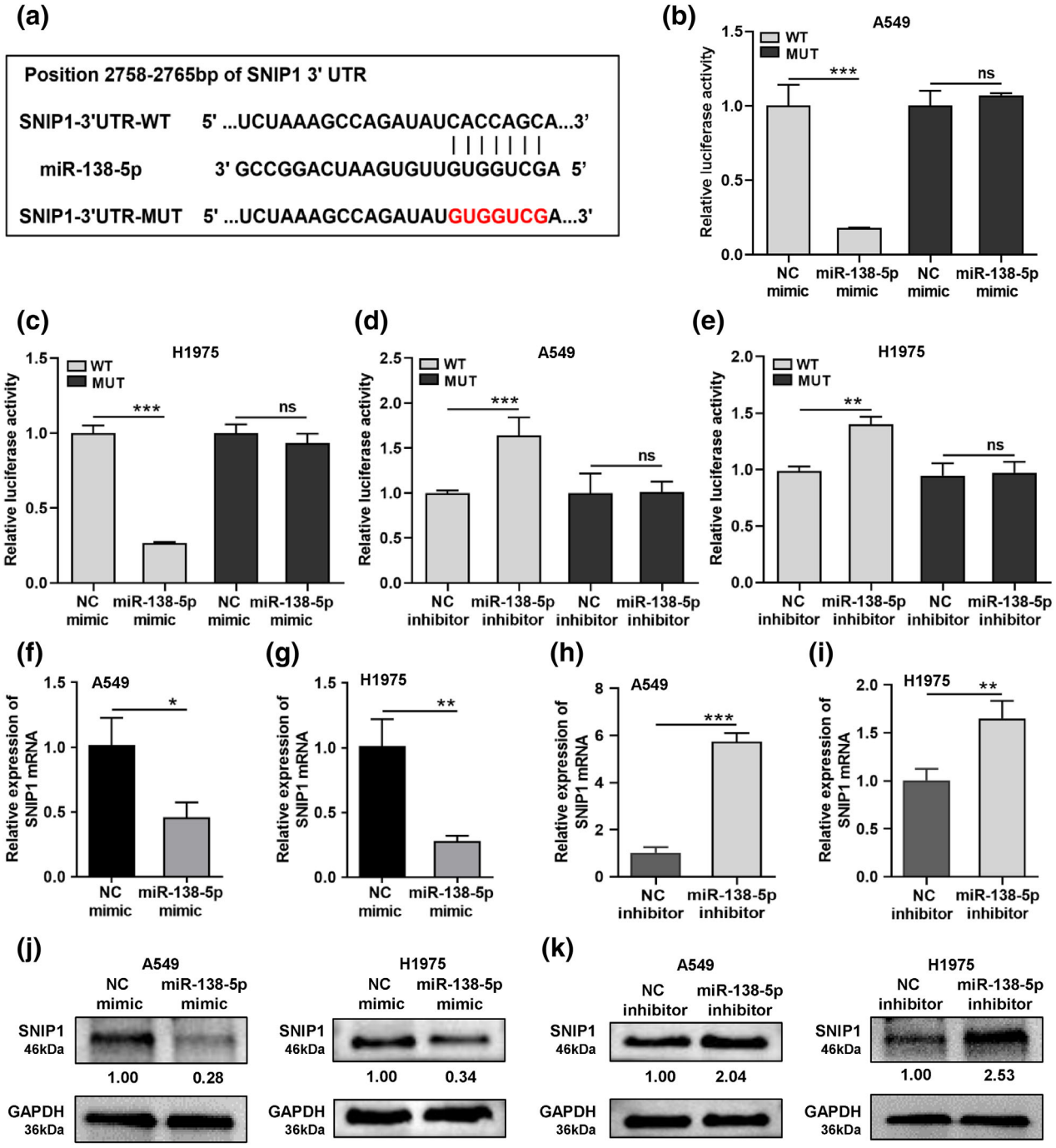

FIGURE 4 SNIP1 is a target gene of miR-138-5p. (a) Graphical presentation of the miR-138-5p putative binding sites in the wild-type and mutant type 3′UTR of SNIP1. (b, c) Luciferase reporter assay was performed following transfection with miR-138-5p mimic or NC mimic using a luciferase vector including the SNIP1 WT 3′UTR or the mutant 3′UTR in A549 or H1975 cells. (d, e) Luciferase reporter assay was performed following transfection with miR-138-5p inhibitor or NC inhibitor using a luciferase vector including the SNIP1 WT 3′UTR or the mutant 3′UTR in A549 or H1975 cells. Luciferase activity was measured 48 h after transfection. All data are presented as the mean ± SD of three independent experiments (**$p < 0.01$; ***$p < 0.001$). (f–i) After transfection of NC mimic, miR-138-5p mimic, NC inhibitor or miR-138-5p inhibitor in the A549 and H1975 cells, the mRNA expression of SNIP1 was detected by RT-qPCR. All data are presented as the mean ± SD of three independent experiments (*$p < 0.05$; **$p < 0.01$; ***$p < 0.001$). (j, k) Protein expression levels of SNIP1 were measured by Western blot after A549 and H1975 cells were transfected with NC mimic, miR-138-5p mimic, NC inhibitor or miR-138-5p inhibitor.

MiR-138-5p suppressed the migration of lung cancer cells

To investigate the role of miR-138-5p in regulating lung cancer cell migration, we transfected the lung cancer cell lines A549 and H1975 with miR-138-5p mimic or miR-138-5p inhibitor and performed transwell migration and wound healing assays. The results showed that miR-138-5p mimic significantly inhibited cell migration of A549 or H1975 cells compared with control treatment

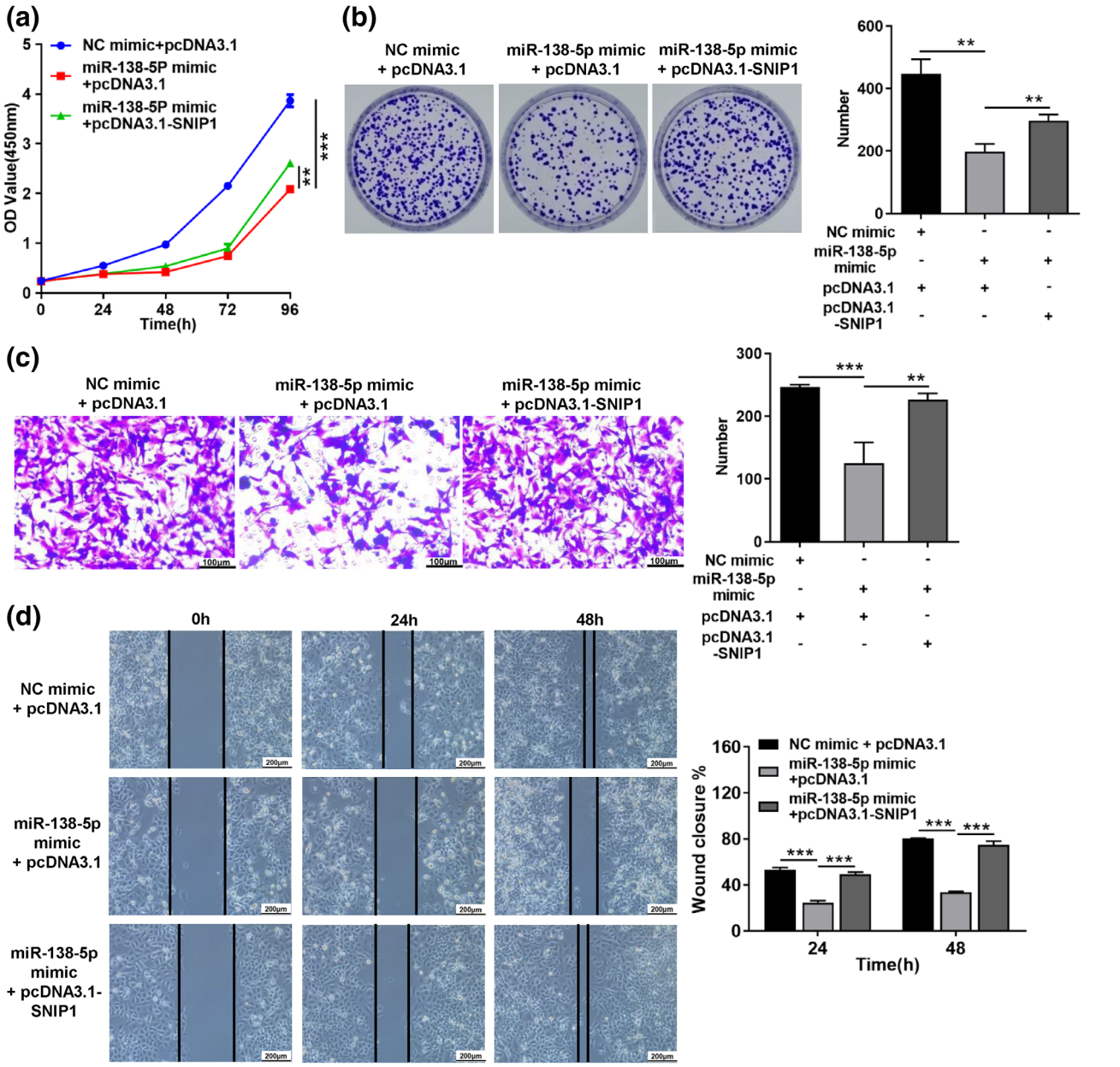

FIGURE 5 Overexpression of SNIP1 rescues the miR-138-5p-mediated inhibition in non-small cell lung cancer (NSCLC) cells. (a) Cell counting kit-8 (CCK-8) assays measured cell proliferation at the indicated time points in A549 cells transfected with NC mimic plus control vector (pcDNA3.1), miR-138-5p mimic plus control vector, or miR-138-5p mimic plus SNIP1 plasmid (pcDNA3.1-SNIP1). (b) Colony formation assays in A549 cells expressing NC mimic plus control vector (pcDNA3.1), miR-138-5p mimic plus control vector, or miR-138-5p mimic plus SNIP1 plasmid (pcDNA3.1-SNIP1) (left panel). Right panel: Quantification of colony formation assays. (c) Transwell analysis of A549 cells transfected with NC mimic plus control vector (pcDNA3.1), miR-138-5p mimic plus control vector, or miR-138-5p mimic plus SNIP1 plasmid (pcDNA3.1-SNIP1). Left panel: Representative images of the migrated cells on the membrane. Right panel: Quantification of transwell migration assay. (d) Representative images of scratch wound healing assays in A549 cells expressing NC mimic plus control vector (pcDNA3.1), miR-138-5p mimic plus control vector, or miR-138-5p mimic plus SNIP1 plasmid (pcDNA3.1-SNIP1) (left panel). Right panel: Quantitative analysis of wound closure. All data are presented as the mean ± SD of three independent experiments (**$p < 0.01$; ***$p < 0.001$)

(Figure 3a,b,e), but miR-138-5p inhibitor increased the metastasis of A549 and H1975 cells compared with control treatment. (Figure 3c,d,f).

Additionally, we sought to determine whether miR-138-5p also regulated the protein expression levels of genes associated with proliferation or migration in lung cancer cells. We transfected lung cancer cells A549 and H1975 with miR-138-5p mimic or miR-138-5p inhibitor and detected the expression of c-Myc, cyclin D1, E-cadherin, and vimentin by Western blot. The results showed that miR-138-5p overexpression could upregulate the protein expression of E-cadherin and downregulate that of c-Myc, cyclin D1 and

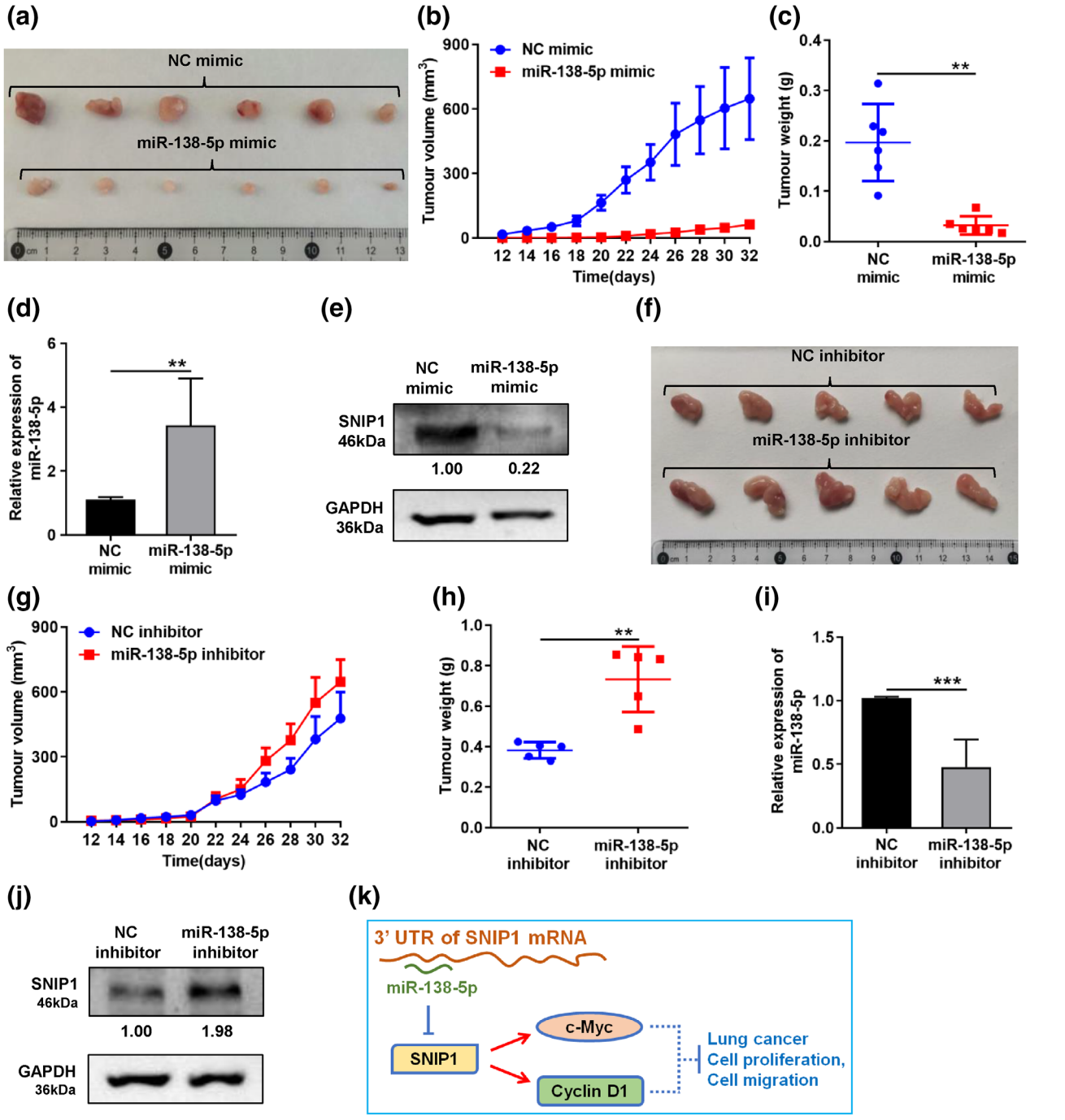

FIGURE 6 MiR-138-5p suppresses the growth of A549 xenograft tumors. Tumorigenesis assay in vivo. The A549 cells (10 million cells per mouse) were treated with lentivirus which overexpressed miR-138-5p mimic or miR-138-5p inhibitor and were injected subcutaneously into 6-week-old female mice. The tumor volume was measured every 2 days. (a, f) Representative images of the excised tumors in the different groups. (b, g) Tumor volume of nude mice. (c, h) Quantitative analysis of the tumor weights on day 32. Data are expressed as median (interquartile range), $^{**}p < 0.01$; Mann-Whitney U test. (d, i) Relative expression of miR-138-5p in xenograft tumors. Values are presented as the mean ± SD of three independent experiments, $^{**}p < 0.01$; $^{***}p < 0.001$. (e, j) Expression levels of SNIP1 in xenograft tumors. (k) Schematic diagram of miR-138-5p and SNIP1 regulating the proliferation and migration of lung cancer cells.

vimentin in A549 and H1975 cells (Figure 3g). MiR-138-5p inhibitor decreased the expression of E-cadherin and increased that of c-Myc, cyclin D1 and vimentin in both cell lines (Figure 3h). Together, these findings indicated that miR-138-5p inhibited the progression of lung cancer.

SNIP1 is a target gene of miR-138-5p

MiRNAs can regulate gene expression by binding to the 3′-untranslated region (UTR) of their target mRNAs.[23] To investigate the mechanism of miR-138-5p in regulating lung

cancer cell proliferation, we predicted the target genes of miR-138-5p by TargetScan and StarBase databases (http://www. targetscan.org/index.html, https://starbase.sysu.edu.cn/). The results showed that the 3′-UTR of SNIP1 mRNA has one binding site for miR-138-5p. Furthermore, SNIP1 was selected as a putative target gene of miR-138-5p because it was reported to be involved in important biological processes in various cancer types.[24,25]

We further investigated whether SNIP1 was a target of miR-138-5p by cloning a 500 bp fragment of the SNIP1 3′UTR. Then, the wild-type SNIP1 3′UTR (Figure 4a) was inserted into the luciferase reporter plasmid and luciferase reporter assay was performed in both cell lines to examine whether miR-138-5p interacts directly with its target SNIP1. We found that the activity of luciferase was markedly reduced in the A549 and H1975 cells cotransfected with the wild-type SNIP1 3′UTR and miR-138-5p mimic compared to the control (Figure 4b,c), but the activity of luciferase was increased in the cells cotransfected with the wild-type SNIP1 3′UTR and miR-138-5p inhibitor compared to the control (Figure 4d,e). Furthermore, we mutated the miR-138-5p binding sites in the 3′UTR fragment of SNIP1 to eliminate the predicted miR-138-5p binding sites (Figure 4a). This mutated luciferase reporter was less affected by either miR-138-5p mimic or miR-138-5p inhibitor (Figure 4b–e). This finding suggested that the binding sites strongly contribute to the interaction between miR-138-5p and SNIP1 mRNA.

We also predicted that at the functional level, miR-138-5p binding to the SNIP1 3′UTR would inhibit SNIP1 expression. We then transfected A549 and H1975 cells with miR-138-5p mimic or miR-138-5p inhibitor. As expected, the miR-138-5p expression significantly increased (Figure 2a,b), whereas the levels of SNIP1 mRNA and protein were downregulated in the A549 and H1975 cells transfected with miR-138-5p mimic (Figure 4f,g,j). Furthermore, the expression of SNIP1 at both RNA and protein levels was upregulated in both cells transfected with miR-138-5p inhibitors (Figure 4h,i,k). In conclusion, miR-138-5p directly recognizes and binds to the 3′-UTR of the SNIP1 mRNA transcript to contribute to the mRNA degradation of this gene in lung cancer cells.

Some studies have demonstrated that SNIP1 may play important roles in several biological processes, including regulating the expression of downstream target genes, such as c-Myc and cyclin D1.[26,27] This study confirmed that miR-138-5p could downregulate the protein expression of c-Myc and cyclin D1 (Figure 3g). Our data demonstrated that miR-138-5p regulated the expression of c-Myc and cyclin D1 by directly targeting SNIP1.

Reconstitution of SNIP1 rescues the miR-138-5p-mediated inhibition in NSCLC cells

To further explore whether SNIP1 can mediate the effects of miR-138-5p on the proliferation and migration in lung cancer cells, we performed rescue experiments by cotransfection of miR-138-5p mimic with or without the SNIP1 overexpression plasmid in A549 cells. As expected, the CCK-8 assay and clone formation assay revealed that cotransfection with both miR-138-5p mimic and the SNIP1 overexpression plasmid could significantly promote the proliferation of A549 cells compared with cells transfected with miR-138-5p mimic alone (Figure 5a,b).

We also evaluated whether SNIP1 overexpression could rescue the suppressive effect of miR-138-5p on cell migration using the transwell migration assay and wound healing assay. A549 cells cotransfected with both miR-138-5p mimic and the SNIP1 overexpression plasmid exhibited significantly higher cell migration rates compared with cells transfected with miR-138-5p mimic alone (Figure 5c,d), suggesting that SNIP1 dramatically attenuated the suppressive effect of miR-138-5p on cell migration.

MiR-138-5p suppresses the growth of A549 xenograft tumors

To explore the effect of miR-138-5p on tumor metastasis in vivo, A549 cells (10 million cells per mouse) treated with lentivirus which overexpressed miR-138-5p mimic or miR-138-5p inhibitor were subcutaneously injected into 6-week-old female nude mice to establish subcutaneous xenograft models. The size and weight of the tumors from the miR-138-5p-overexpressing group were decreased compared to those of the control groups (Figure 6a–c). As expected, miR-138-5p was overexpressed but SNIP1 was reduced in the miR-138-5p-overexpressing group compared with the control groups (Figure 6d,e). By contrast, the size and weight of the tumors in the group implanted with cells containing the miR-138-5p inhibitor were increased (Figure 6f–h). MiR-138-5p also was decreased and SNIP1 was increased in miR-138-5p inhibitor-treated xenografts compared with the control groups (Figure 6i,j). These results suggested that miR-138-5p inhibited the proliferation and metastasis of lung cancer cells in vivo.

DISCUSSION

Serum tumor markers are among the most commonly used detection methods for malignant tumors. The stable miRNAs in peripheral blood are expected to become noninvasive cancer detection markers. Previous studies have shown that miRNAs can be considered as diagnostic biomarkers for NSCLC.[7,11] For example, Ulivi et al. found that the expression of miR-328 in peripheral blood can be used as a potential biomarker for the early diagnosis of NSCLC.[28] Our recent findings showed that miR-138-5p was downregulated in the NSCLC serum as well as in the NSCLC cells. MiR-138-5p downregulation has also been reported in other cancers.[16,22] ROC analysis revealed that miR-138-5p in NSCLC may be a promising diagnostic biomarker (Figure 1b).

MiR-138-5p plays important roles in the carcinogenesis of NSCLC as a tumor suppressor. As is well known, a single miRNA can target multiple genes. For example, miR-138

inhibits NSCLC cell growth and reverses epithelial-mesenchymal transition (EMT) in NSCLC cells by targeting GIT1 and SEMA4C.[8] MiR-138 suppresses the proliferation and metastasis of NSCLC by targeting Sirt1.[9] MiR-138-5p suppresses the growth of NSCLC cells by targeting PD-1/PD-L1 and regulates the tumor microenvironment.[10] However, the biological function of miR-138-5p in NSCLC has not yet been completely elucidated. In our study, various functional experiments suggested that overexpression of the miR-138-5p vitally inhibits the proliferation and migration of the NSCLC cells (Figures 2 and 3). Specifically, the miR-138-5p obviously inhibited the proliferation and metastasis of lung cancer cells in vivo (Figure 6). Our research proved that miR-138-5p could downregulate SNIP1 expression levels by binding directly to the potential target site of SNIP1 mRNA 3′UTR in NSCLC cells, indicating that SNIP1 is a novel target of miR-138-5p.

As an evolutionarily conserved nuclear protein, SNIP1 is a transcription regulator and plays a key role in tumor development and progression.[25,26,29–31] SNIP1 is involved in miRNA biogenesis,[32] cell proliferation and differentiation,[31,33,34] DNA damage response,[27] and several signaling pathways.[29,30] In addition, lncRNA AFAP1-AS1 promoted lung cancer cell migration and invasion through interacting with SNIP1 to upregulate c-Myc.[35] It is well known that a single gene can be regulated by multiple miRNAs. Recently, SNIP1 was reported to be targeted by miR-335 and overexpression of SNIP1 promoted cell proliferation and metastasis in osteosarcoma cells.[36] SNIP1 was also targeted by miR-29a-3p and influenced the migration and proliferation of cervical cancer HeLa cells.[37] High expression of SNIP1 has been identified as a poor prognostic indicator in NSCLC.[24] However, the function of SNIP1 in the development of NSCLC remains obscure. Interestingly, we further observed that the restoration of SNIP1 expression can reverse the antiproliferative and antimigration effect of miR-138-5p on NSCLC cells (Figure 5), although miR-138-5p have many other potential targets. Altogether, we conclude that miR-138-5p can modulate NSCLC cell growth by suppressing the expression of SNIP1.

As previously described in the literature, SNIP1 could regulate the transcriptional activity of c-Myc[27,31] and the stability of cyclin D1 mRNA.[26] These downstream genes (c-Myc and cyclin D1) regulated by SNIP1 are considered to be closely involved in cell proliferation and migration.[38–40] In this research, miR-138-5p decreased the protein expression levels of c-Myc and cyclin D1 in NSCLC cells as an upstream regulator. Therefore, miR-138-5p suppressed the proliferation and migration of NSCLC cells by negatively regulating a novel target SNIP1, thereby further affecting the expression of c-Myc and cyclin D1 (Figure 6k). Additional research is required to reveal the underlying mechanism of the miR-138-5p/SNIP1 pathway in NSCLC oncogenesis.

In summary, miR-138-5p is useful as a diagnostic biomarker for NSCLC. This study demonstrated that miR-138-5p could suppress the proliferation and migration of NSCLC cells by negatively regulating SNIP1.

AUTHOR CONTRIBUTIONS

Hongfang Sun, Shuyang Xie, and Jiankai Feng designed the study, performed data analysis, and revised the manuscript. Xiancong Yang and Youjie Li collected clinical samples. Jiaen Wu and Xuejia Han performed cell culture, miRNA detection, cell proliferation, cell migration and luciferase assay. Guangbin Sun and Yan Liang performed the immunoblotting assay. Pingyu Wang and Ranran Wang produced xenografts in vivo. All authors approved the final manuscript.

ACKNOWLEDGMENTS

This work was supported by the National Natural Science Foundation of China (grant no. 82002604), the Natural Science Foundation of Shandong (grant nos. ZR2020QH221, ZR2019MH022, ZR2019PH061, and ZR2020KH015), the Support Plan For Youth Entrepreneurship and Technology of Colleges and Universities in Shandong (grant nos. 2021KJ101, 2019KJK014), and the Scientific Research Foundation of Binzhou Medical University (project no. 50012304278), and the Shandong Province Taishan Scholar Project (grant no. ts201712067).

CONFLICT OF INTEREST

The authors declare no conflicts of interest.

ETHICS STATEMENT

The study protocol was approved by the Medical Ethics Committee of Binzhou Medical University.

ORCID

Shuyang Xie https://orcid.org/0000-0002-8090-2180
Hongfang Sun https://orcid.org/0000-0002-4322-4851

REFERENCES

1. Sung H, Ferlay J, Siegel RL, Laversanne M, Soerjomataram I, Jemal A, et al. Global cancer statistics 2020: GLOBOCAN estimates of incidence and mortality worldwide for 36 cancers in 185 countries. CA Cancer J Clin. 2021;71(3):209–49.
2. Lei ZN, Teng QX, Zhang W, Fan YF, Wang JQ, Cai CY, et al. Establishment and characterization of a Topotecan resistant non-small cell lung cancer NCI-H460/TPT10 cell line. Front Cell Dev Biol. 2020;8:607275.
3. Bernardo BC, Ooi JY, Lin RC, McMullen JR. miRNA therapeutics: a new class of drugs with potential therapeutic applications in the heart. Future Med Chem. 2015;7(13):1771–92.
4. Javadian M, Gharibi T, Shekari N, Abdollahpour-Alitappeh M, Mohammadi A, Hossieni A, et al. The role of microRNAs regulating the expression of matrix metalloproteinases (MMPs) in breast cancer development, progression, and metastasis. J Cell Physiol. 2019;234(5):5399–412.
5. Baradaran B, Shahbazi R, Khordadmehr M. Dysregulation of key microRNAs in pancreatic cancer development. Biomed Pharmacother. 2019;109:1008–15.
6. Chen X, Hu Z, Wang W, Ba Y, Ma L, Zhang C, et al. Identification of ten serum microRNAs from a genome-wide serum microRNA expression profile as novel noninvasive biomarkers for nonsmall cell lung cancer diagnosis. Int J Cancer. 2012;130(7):1620–8.
7. Ying L, Du L, Zou R, Shi L, Zhang N, Jin J, et al. Development of a serum miRNA panel for detection of early stage non-small cell lung cancer. Proc Natl Acad Sci USA. 2020;117(40):25036–42.
8. Li J, Wang Q, Wen R, Liang J, Zhong X, Yang W, et al. MiR-138 inhibits cell proliferation and reverses epithelial-mesenchymal

transition in non-small cell lung cancer cells by targeting GIT1 and SEMA4C. J Cell Mol Med. 2015;19(12):2793–805.
9. Ye Z, Fang B, Pan J, Zhang N, Huang J, Xie C, et al. miR-138 suppresses the proliferation, metastasis and autophagy of non-small cell lung cancer by targeting Sirt1. Oncol Rep. 2017;37(6):3244–52.
10. Song N, Li P, Song P, Li Y, Zhou S, Su Q, et al. MicroRNA-138-5p suppresses non-small cell lung cancer cells by targeting PD-L1/PD-1 to regulate tumor microenvironment. Front Cell Dev Biol. 2020; 8:540.
11. Asakura K, Kadota T, Matsuzaki J, Yoshida Y, Yamamoto Y, Nakagawa K, et al. A miRNA-based diagnostic model predicts resectable lung cancer in humans with high accuracy. Commun Biol. 2020;3(1):134.
12. Cohen JD, Li L, Wang Y, Thoburn C, Afsari B, Danilova L, et al. Detection and localization of surgically resectable cancers with a multi-analyte blood test. Science. 2018;359(6378):926–30.
13. Sozzi G, Boeri M, Rossi M, Verri C, Suatoni P, Bravi F, et al. Clinical utility of a plasma-based miRNA signature classifier within computed tomography lung cancer screening: a correlative MILD trial study. J Clin Oncol. 2014;32(8):768–73.
14. Montani F, Marzi MJ, Dezi F, Dama E, Carletti RM, Bonizzi G, et al. miR-test: a blood test for lung cancer early detection. J Natl Cancer Inst. 2015;107(6):djv063.
15. Sun H, He L, Wu H, Pan F, Wu X, Zhao J, et al. The FEN1 L209P mutation interferes with long-patch base excision repair and induces cellular transformation. Oncogene. 2017;36(2):194–207.
16. Yang R, Liu M, Liang H, Guo S, Guo X, Yuan M, et al. miR-138-5p contributes to cell proliferation and invasion by targeting Survivin in bladder cancer cells. Mol Cancer. 2016;15(1):82.
17. Liu T, Li T, Zheng Y, Xu X, Sun R, Zhan S, et al. Evaluating adipose-derived stem cell exosomes as miRNA drug delivery systems for the treatment of bladder cancer. Cancer Med. 2022;11(19):3687–99.
18. Chen LY, Wang L, Ren YX, Pang Z, Liu Y, Sun XD, et al. The circular RNA circ-ERBIN promotes growth and metastasis of colorectal cancer by miR-125a-5p and miR-138-5p/4EBP-1 mediated cap-independent HIF-1alpha translation. Mol Cancer. 2020;19(1):164.
19. Zhang Y, Sun Y, Ding L, Shi W, Ding K, Zhu Y. Long non-coding RNA LINC00467 correlates to poor prognosis and aggressiveness of breast cancer. Front Oncol. 2021;11:643394.
20. Zhang S, Lu Y, Jiang HY, Cheng ZM, Wei ZJ, Wei YH, et al. CircC16orf62 promotes hepatocellular carcinoma progression through the miR-138-5p/PTK2/AKT axis. Cell Death Dis. 2021;12(6):597.
21. Bai B, Liu Y, Fu XM, Qin HY, Li GK, Wang HC, et al. Dysregulation of EZH2/miR-138-5p Axis contributes to Radiosensitivity in hepatocellular carcinoma cell by downregulating hypoxia-inducible factor 1 alpha (HIF-1alpha). Oxid Med Cell Longev. 2022;2022:7608712.
22. Zhang D, Liu X, Zhang Q, Chen X. miR-138-5p inhibits the malignant progression of prostate cancer by targeting FOXC1. Cancer Cell Int. 2020;20:297.
23. Zhang K, Zhang X, Cai Z, Zhou J, Cao R, Zhao Y, et al. A novel class of microRNA-recognition elements that function only within open reading frames. Nat Struct Mol Biol. 2018;25(11):1019–27.
24. Jeon HS, Choi YY, Fukuoka J, Fujii M, Lyakh LA, Song SH, et al. High expression of SNIP1 correlates with poor prognosis in non-small cell lung cancer and SNIP1 interferes with the recruitment of HDAC1 to RB in vitro. Lung Cancer. 2013;82(1):24–30.
25. Yu B, Su J, Shi Q, Liu Q, Ma J, Ru G, et al. KMT5A-methylated SNIP1 promotes triple-negative breast cancer metastasis by activating YAP signaling. Nat Commun. 2022;13(1):2192.
26. Bracken CP, Wall SJ, Barre B, Panov KI, Ajuh PM, Perkins ND. Regulation of cyclin D1 RNA stability by SNIP1. Cancer Res. 2008;68(18): 7621–8.
27. Chen LL, Lin HP, Zhou WJ, He CX, Zhang ZY, Cheng ZL, et al. SNIP1 recruits TET2 to regulate c-MYC target genes and cellular DNA damage response. Cell Rep. 2018;25(6):1485–500 e4.
28. Ulivi P, Foschi G, Mengozzi M, Scarpi E, Silvestrini R, Amadori D, et al. Peripheral blood miR-328 expression as a potential biomarker for the early diagnosis of NSCLC. Int J Mol Sci. 2013;14(5):10332–42.
29. Kim RH, Wang D, Tsang M, Martin J, Huff C, de Caestecker MP, et al. A novel Smad nuclear interacting protein, SNIP1, suppresses p300-dependent TGF-β signal transduction. Genes Dev. 2000;14(13): 1605–16.
30. Kim RH, Flanders KC, Birkey Reffey S, Anderson LA, Duckett CS, Perkins ND, et al. SNIP1 inhibits NF-kappa B signaling by competing for its binding to the C/H1 domain of CBP/p300 transcriptional coactivators. J Biol Chem. 2001;276(49):46297–304.
31. Fujii M, Lyakh LA, Bracken CP, Fukuoka J, Hayakawa M, Tsukiyama T, et al. SNIP1 is a candidate modifier of the transcriptional activity of c-Myc on E box-dependent target genes. Mol Cell. 2006;24(5):771–83.
32. Yu B, Bi L, Zheng B, Ji L, Chevalier D, Agarwal M, et al. The FHA domain proteins DAWDLE in Arabidopsis and SNIP1 in humans act in small RNA biogenesis. Proc Natl Acad Sci U S A. 2008;105(29): 10073–8.
33. Roche KC, Wiechens N, Owen-Hughes T, Perkins ND. The FHA domain protein SNIP1 is a regulator of the cell cycle and cyclin D1 expression. Oncogene. 2004;23(50):8185–95.
34. Yang Z, Song C, Jiang R, Huang Y, Lan X, Lei C, et al. Micro-ribonucleic acid-216a regulates bovine primary muscle cells proliferation and differentiation via targeting SMAD nuclear interacting Protein-1 and Smad7. Front Genet. 2019;10:1112.
35. Zhong Y, Yang L, Xiong F, He Y, Tang Y, Shi L, et al. Long non-coding RNA AFAP1-AS1 accelerates lung cancer cells migration and invasion by interacting with SNIP1 to upregulate c-Myc. Signal Transduct Target Ther. 2021;6(1):240.
36. Xie Y, Deng H, Wei R, Sun W, Qi Y, Yao S, et al. Overexpression of miR-335 inhibits the migration and invasion of osteosarcoma by targeting SNIP1. Int J Biol Macromol. 2019;133:137–47.
37. Chen Y, Zhang W, Yan L, Zheng P, Li J. miR-29a-3p directly targets Smad nuclear interacting protein 1 and inhibits the migration and proliferation of cervical cancer HeLa cells. PeerJ. 2020;8:e10148.
38. Evan G, Harrington E, Fanidi A, Land H, Amati B, Bennett M. Integrated control of cell proliferation and cell death by the c-myc oncogene. Philos Trans R Soc Lond B Biol Sci. 1994;345(1313):269–75.
39. Li Q, An J, Liu X, Zhang M, Ling Y, Wang C, et al. SNIP1: a new activator of HSE signaling pathway. Mol Cell Biochem. 2012;362(1–2):1–6.
40. Pestell RG. New roles of cyclin D1. Am J Pathol. 2013;183(1):3–9.

How to cite this article: Wu J, Han X, Yang X, Li Y, Liang Y, Sun G, et al. MiR-138-5p suppresses the progression of lung cancer by targeting SNIP1. Thorac Cancer. 2023;14(6):612–23. https://doi.org/10.1111/1759-7714.14791